

# Photoinduced Charge Separation and Charge Recombination in [60]Fullerene-(Benzothiadiazole-Triphenylamine) Based Dyad in Polar Solvents

Atula S. D. Sandanayaka,<sup>†</sup> Kyohei Matsukawa,<sup>‡</sup> Tsutomu Ishi-i,<sup>\*,§</sup> Shuntaro Mataka,<sup>\*,§</sup> Yasuyuki Araki,<sup>†</sup> and Osamu Ito<sup>\*,†</sup>

*Institute of Multidisciplinary Research for Advanced Materials, Tohoku University, Katahira 2-1-1, Aoba-ku, Sendai 980-8577, Japan, Interdisciplinary Graduate School of Engineering Sciences, Kyushu University, 6-1 Kasuga-kohen, Kasuga 816-8580, Japan, and Institute for Materials Chemistry and Engineering (IMCE), Kyushu University, 6-1 Kasuga-kohen, Kasuga 816-8580, Japan*

*Received: October 1, 2004*

The molecular dyad C<sub>60</sub>-(BTD-TPA) consisting of an electron donor triphenylamine-appended 2,1,3-benzothiadiazole chromophore (BTD-TPA) unit covalently linked to an electron acceptor [60]fullerene has been synthesized. The photoinduced electron transfer in C<sub>60</sub>-(BTD-TPA) has been studied in polar and nonpolar solvents using time-resolved transient absorption and fluorescence measurements. By fluorescence lifetime measurements in picosecond time regions, the excitation of the C<sub>60</sub> moiety leads to the formation of C<sub>60</sub><sup>•−</sup>-(BTD-TPA)<sup>•+</sup> efficiently via the singlet excited state of the C<sub>60</sub> moiety. Excitation of the BTD-TPA moiety leads to initial energy transfer to <sup>1</sup>C<sub>60</sub><sup>\*</sup>-(BTD-TPA), from which electron transfer occurs to form C<sub>60</sub><sup>•−</sup>-(BTD-TPA)<sup>•+</sup>. In the nanosecond time region, C<sub>60</sub><sup>•−</sup>-(BTD-TPA)<sup>•+</sup> in which the radical cation (hole) delocalizes in the BTD-TPA moiety is persistent for 690 ns in DMF at room temperature. From the temperature dependence of the charge-recombination rate constants, which gave the Marcus parameters, we attempted to reveal the origins of long persistent C<sub>60</sub><sup>•−</sup>-(BTD-TPA)<sup>•+</sup> in DMF.

## Introduction

For the past decade, fullerene derivatives were developed to be remarkable building blocks for the design of new photochemical molecular devices.<sup>1–6</sup> Fullerene derivatives covalently bound to electron donors have been synthesized, and photochemical and photophysical properties have been investigated. In these molecular systems, fullerenes act as efficient electron acceptors, exhibiting photoinduced intramolecular electron transfer.<sup>1–6</sup> Photoexcitation of either electron donor or C<sub>60</sub> of the dyad leads to an electron transfer to form the radical anion of C<sub>60</sub> and the radical cation of the electron donor. The efficiencies and rates of electron-transfer processes in the C<sub>60</sub> based dyads and triads can be tuned by the energy of the donor-C<sub>60</sub> pair, distances, and orientations between the electron donor and C<sub>60</sub> moieties.<sup>1–6</sup> Then, it has been revealed that the fullerene sphere is a particularly interesting electron acceptor of its small reorganization energy due to its symmetrical shape, its large size, and its unique  $\pi$ -electron system.<sup>7</sup> Thus, efficient charge separation (CS) and slow charge recombination (CR) have been achieved, serving appropriated artificial photosynthetic models.<sup>8</sup> A number of fullerene based dyads and triads containing olefins,<sup>9</sup> dimethylanilines,<sup>10</sup> porphyrins,<sup>11</sup> phthalocyanines,<sup>12</sup> ruthenium complexes,<sup>13</sup> ferrocenes,<sup>14</sup> tetrathiafluvalenes,<sup>15</sup> and oligothiophene<sup>16</sup> as electron donors were synthesized. In these dyads and triads, the importance of sensitizing donors and acceptors, from which the CS process takes place, generating the radical cation (hole) and radical anion (electron) has been

reported. In addition, the important roles of the bridged molecules connecting electron donors and acceptors have been pointed out.<sup>17</sup> In our previous papers,<sup>18,19</sup> we reported that the bridge molecular units to connect the C<sub>60</sub> moiety and the donor molecules play a role to assist the electron donor ability and hole delocalization.

4,7-Diphenyl-2,1,3-benzothiadiazole and its derivatives are known as strongly fluorescent dyes.<sup>20,21</sup> The absorption and emitting bands can be tuned by the aromatic substituents introduced at the 4 and 7 positions of the benzothiadiazole core. Further, the benzothiadiazole unit was used as an important spacer in semiconducting oligomers.<sup>22</sup> Recently, one of our groups has developed the benzothiadiazole dyes to functional materials such as dichroic fluorescent materials<sup>23</sup> and red-fluorescent two-photon-absorbing materials.<sup>24</sup>

In the present study, we have synthesized a dyad in which 2,1,3-benzothiadiazole (BTD) is covalently bonded to triphenylamine (TPA) used as a combined electron donor, to which C<sub>60</sub> is covalently linked at one end of BTD-TPA as shown in Figure 1 (abbreviated as C<sub>60</sub>-(BTD-TPA)). The BTD moiety was selected expecting to act also as a bridge because of its relatively high LUMO energy.<sup>25</sup> The BTD moiety is strongly coupled with the TPA moiety to form a chromophore acting as a light-harvesting antenna.

Our aim of the present study is to measure the rates and efficiencies of the CS processes by time-resolved fluorescence measurements with changing solvent polarity and excitation wavelengths; one is C<sub>60</sub> excitation and another is BTD-TPA excitation. The nanosecond lifetimes of the CS states were measured with the transient spectra measurements. The origin of the long lifetimes of the CS state has been revealed by the Marcus parameters experimentally evaluated from the temperature dependence of the CR rate constants.<sup>26</sup>

\* To whom correspondence should be addressed. E-mail: ishi-i@cm.kyushu-u.ac.jp.

<sup>†</sup> Tohoku University.

<sup>‡</sup> Interdisciplinary Graduate School of Engineering Sciences, Kyushu University.

<sup>§</sup> IMCE, Kyushu University.

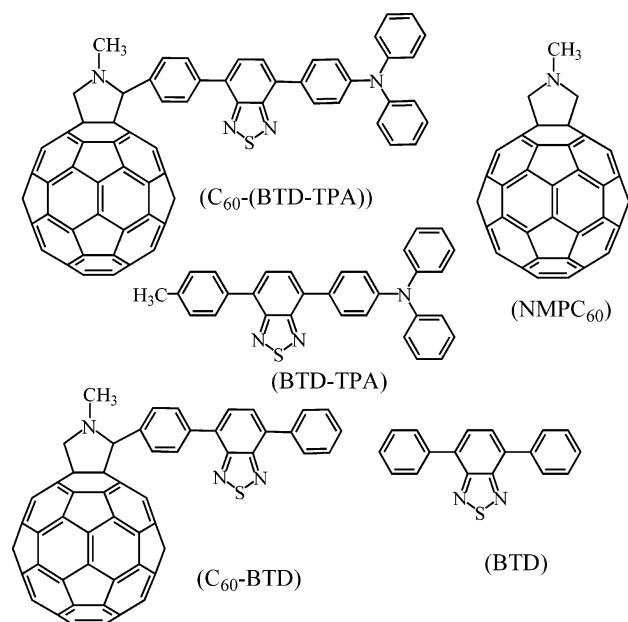


**Figure 1.** Molecular structures of  $C_{60}$ -(BTD-TPA) and reference compounds.

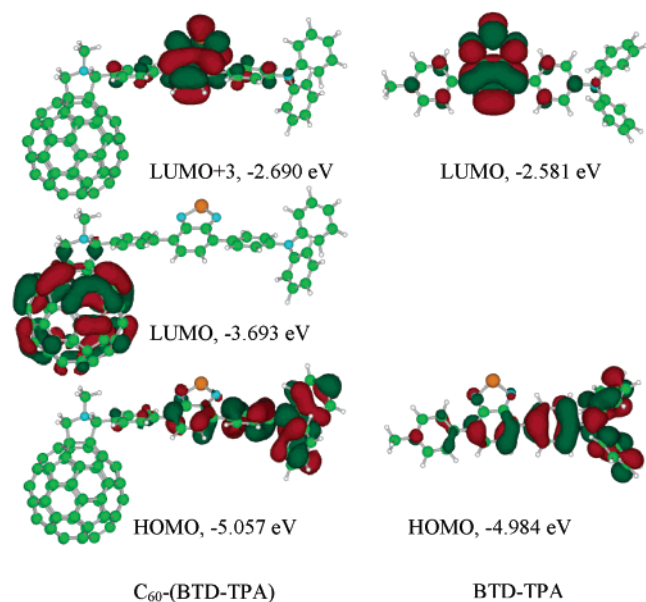


**Figure 2.** Frontier HOMO and LUMO's of  $C_{60}$ -(BTD-TPA) and BTD-TPA calculated by density function B3LYP/3-21G(\*) methods.

## Results and Discussion

**Synthesis.**  $C_{60}$ -(BTD-TPA) dyad and its reference compound BTD-TPA were prepared as shown in Scheme 1, in which Suzuki coupling reaction and Prato reaction were used as key steps.<sup>27</sup> The reference compound  $C_{60}$ -BTD without terminal diphenylamino groups was similarly prepared (Scheme 1).  $C_{60}$ -(BTD-TPA),  $C_{60}$ -BTD and BTD-TPA were identified on the basis of spectroscopic methods and elemental analysis (see Experimental Section).

**Molecular Orbital Calculations.** To gain insights into the molecular geometries and electronic structures of  $C_{60}$ -(BTD-TPA) and BTD-TPA, MO calculations were performed using density function B3LYP/3-21G(\*) method.<sup>28</sup> For these MO calculations, the starting compounds were fully optimized to a stationary point on the Born-Openheimer potential energy surface. The geometric parameters of the compounds were obtained after completing energy minimization. The optimized

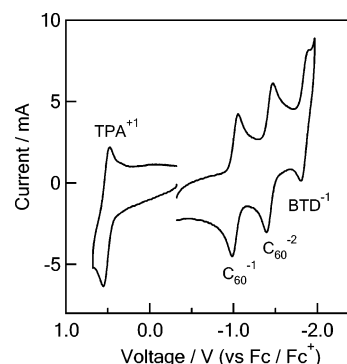


**Figure 3.** Cyclic voltammograms of  $C_{60}$ -(BTD-TPA) (0.5 mM) in the presence of tetra-*n*-butylammonium perchlorate (0.1 M) in PhCN. Scan rate = 100 mV s<sup>-1</sup>.

**TABLE 1: Cyclic Voltammetry Data of  $C_{60}$ -(BTD-TPA) and BTD-TPA**

compounds	solvents	V vs Fc/Fc <sup>+</sup>				
		E <sub>ox</sub> (BTD-TPA)	E <sub>red</sub> (C <sub>60</sub> )	E <sub>red</sub> (C <sub>60</sub> )	E <sub>red</sub> (BTD-TPA)	E <sub>red</sub> (C <sub>60</sub> )
$C_{60}$ -(BTD-TPA)	PhCN	0.51	-1.03	-1.44	-1.85	-
BTD-TPA	PhCN	0.50			-1.88	-
$C_{60}$ -(BTD-TPA)	DMF	0.53	-0.91	-1.36	-1.78	-2.03
BTD-TPA	DMF	0.53			-1.79	

structures are shown in Figure 2. The center-to-center distances ( $R_{CC}$ ) between  $C_{60}$ -TPA,  $C_{60}$ -BTD, and BTD-TPA moieties were estimated to be 22, 13, and 7 Å from the optimized structure of  $C_{60}$ -(BTD-TPA).

Furthermore, Figure 2 shows the spatial electron distributions for the HOMO, LUMO, and LUMO+3 of  $C_{60}$ -(BTD-TPA) and the HOMO and LUMO for BTD-TPA. In these compounds, the majority of the electron distributions of HOMO were found to be located on the TPA moiety with a small orbital coefficient on the BTD moiety. It can be clearly seen from Figure 2 that the LUMO for  $C_{60}$ -(BTD-TPA) localizes on the  $C_{60}$  spheroid. The LUMO+1 and LUMO+2, which have almost similar energy levels to that of the LUMO, also localize on the  $C_{60}$  spheroid. The LUMO+3, which has higher energy than the LUMO, localizes on the BTD moiety. In the case of BTD-TPA, the majority of the electron distribution of the LUMO locates on the BTD moiety in BTD-TPA, whereas the HOMO mainly delocalizes on the BTD-TPA. It is interesting to note here that the observed energy level difference between LUMO and LUMO+3 (1 eV) is similar to the experimentally observed energy difference between excited singlet states of  $C_{60}$  and BTD-TPA (0.7 eV).

**Electrochemical Studies.** The electrochemical properties of  $C_{60}$ -(BTD-TPA), NMP- $C_{60}$ , and BTD-TPA have been studied by cyclic voltammetry measurements in benzonitrile (PhCN) and DMF at room temperature (Figure 3). From the reversible peaks of  $C_{60}$ -(BTD-TPA), the reduction ( $E_{red}$ ) and oxidation potentials ( $E_{ox}$ ) were evaluated at -0.91, -1.36, -1.78, and +0.53 V vs Fc/Fc<sup>+</sup> in DMF. The first and second negative potentials are attributed to the  $E_{red}$  values of the  $C_{60}$  moiety, the third negative potential is attributed to the  $E_{red}$  value of the BTD moiety connected with TPA moiety, and positive potential is assigned to the  $E_{ox}$  value of the TPA moiety connected with BTD in  $C_{60}$ -BTD-TPA by comparing the  $E_{red}$  and  $E_{ox}$  values of reference compounds as listed in Table 1. The electrochemical studies confirm that there is no appreciable electronic interaction between the  $C_{60}$  and the BTD-TPA moieties in the ground state.

The energy levels ( $\Delta G_{RP}^0$ ) of the radical ion-pair ( $C_{60}^{\bullet-}$ -(BTD-TPA)<sup>•+</sup>), which are equal to the free-energy changes of

## SCHEME 1

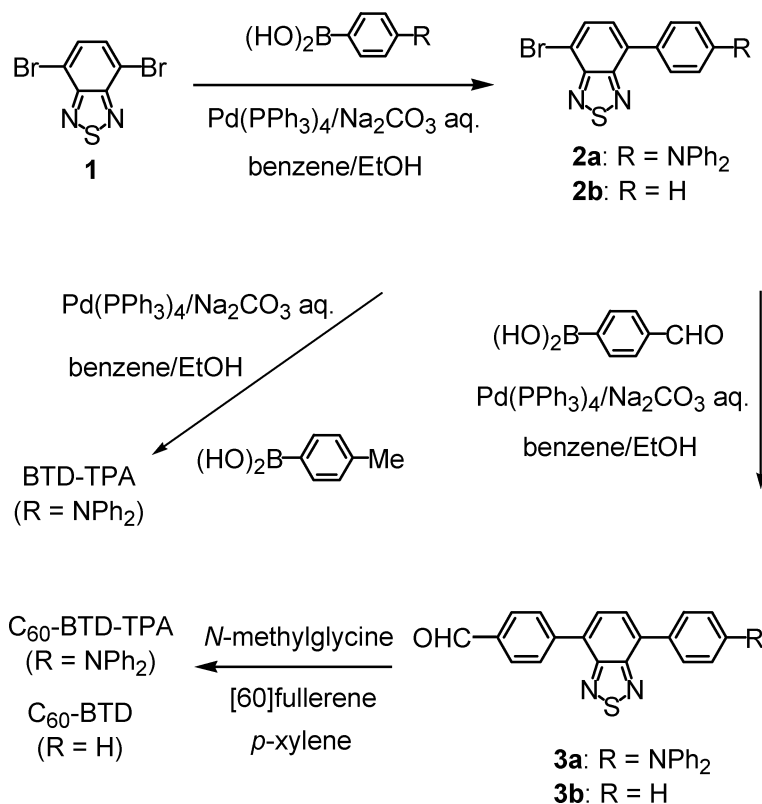


**TABLE 2: Fluorescence Lifetimes ( $\tau$ ), Rate Constant ( $k_{CS}$ ),<sup>a</sup> the Quantum Yield ( $\Phi_{CS}$ ),<sup>a</sup> and Free-Energy Changes of Charge Separation ( $\Delta G_{CS}^0$ ) and Charge Recombination ( $\Delta G_{CR}^0$ ) of C<sub>60</sub>-(BTD-TPA) in Toluene, PhCN, and DMF at Room Temperature**

compounds	solvents	$\tau$ /ps	$k_{CS}^a/s^{-1}$	$\Phi_{CS}^a$	$-\Delta G_{CS}^0$ /eV	$-\Delta G_{CR}^0$ /eV
<sup>1</sup> C <sub>60</sub> *(BTD-TPA) <sup>c</sup>	toluene	1480			-0.52 <sup>d</sup>	2.27
<sup>1</sup> C <sub>60</sub> *(BTD-TPA) <sup>c</sup>	PhCN	570	$1.1 \times 10^{10d}$	0.62 <sup>d</sup>	0.24 <sup>d</sup>	1.51
<sup>1</sup> C <sub>60</sub> *(BTD-TPA) <sup>c</sup>	DMF	290 <sup>e</sup>	$2.8 \times 10^{10d}$	0.81 <sup>d</sup>	0.33 <sup>d</sup>	1.42
C <sub>60</sub> - <sup>1</sup> (BTD-TPA)* <sup>c</sup>	toluene	50 <sup>e</sup>	$(2.0 \times 10^{10})^f$	(0.99) <sup>f</sup>	-0.04 <sup>g</sup>	2.27
C <sub>60</sub> - <sup>1</sup> (BTD-TPA)* <sup>c</sup>	PhCN	30 <sup>e</sup>	$1.3 \times 10^{10g}$	0.39 <sup>g</sup>	0.43 <sup>g</sup>	1.51
C <sub>60</sub> - <sup>1</sup> (BTD-TPA)* <sup>c</sup>	DMF	30 <sup>e</sup>	$1.3 \times 10^{10g}$	0.39 <sup>g</sup>	0.47 <sup>g</sup>	1.42

<sup>a</sup> Calculated by eqs 3 and 4, ( $\tau_{ref}$ ) were employed to be 1480 ps for NMPC<sub>60</sub> and 7000 ps for BTD-TPA (in toluene). <sup>b</sup>  $\Delta G_{CS}^0$  was calculated from the Weller eqs 1 and 2.  $\Delta G_S = e^2/(4\pi\epsilon_0)[(1/(2R_+) + 1/(2R_-) - 1/R_{cc})/\epsilon_R - (1/(2R_+) + 1/(2R_-))/\epsilon_R]$ , where  $R_+$  and  $R_-$  and  $R_{cc}$  are radii of cation and anion, and center-to-center distance between donor and acceptor, respectively. The  $\epsilon_R$  is dielectric constants of solvents used for measuring the redox potentials.<sup>24</sup> <sup>c</sup> Fluorescence decays of C<sub>60</sub> and (BTD-TPA). <sup>d</sup> CS via <sup>1</sup>C<sub>60</sub>\* ( $k_{CS}^1$  and  $\Phi_{CS}^1$ ). <sup>e</sup> Fluorescence decay (<sup>1</sup>C<sub>60</sub>\*) in DMF was fitted with biexponential decays [290 ps (85%) and 1400 ps (15%)];  $k_{CS}$  and  $\Phi_{CS}$  were calculated from the shorter lifetimes. Fluorescence decays of <sup>1</sup>(BTD-TPA)\* were fitted with biexponential decays giving 50 ps (80%) and 5020 ps (20%) in toluene, 30 ps (94%) and 4760 ps (6%) in PhCN, and 30 ps (92%) and 4880 ps (8%) in DMF. <sup>f</sup> EN via <sup>1</sup>(BTD-TPA)\* to C<sub>60</sub> ( $k_{EN}$  and  $\Phi_{EN}$ ). <sup>g</sup> CS via C<sub>60</sub>-<sup>1</sup>(BTD-TPA)\* ( $k_{CS}^{II}$  and  $\Phi_{CS}^{II}$ ).

charge-recombination ( $\Delta G_{CR}^0$ ), were evaluated as a difference between the  $E_{ox}$  and  $E_{red}$  values, considering the Coulomb energy ( $\Delta G_S$ ) by the Weller equations.<sup>29</sup> The free energy changes for charge-separation ( $\Delta G_{CS}^0$ ) can be calculated by considering the energy levels of the lowest excited states of the C<sub>60</sub> and BTD-TPA moiety<sup>29</sup>

$$\Delta G_{RIP}^0 = -\Delta G_{CR}^0 = -E_{ox} + E_{red} - \Delta G_S \quad (1)$$

$$-\Delta G_{CS}^0 = \Delta E_{0-0} - \Delta G_{RIP}^0 \quad (2)$$

In eqs 1 and 2,  $\Delta E_{0-0}$  refers to the lowest excited states of the C<sub>60</sub> (1.75 eV) and BTD-TPA (2.23 eV).<sup>29</sup> The calculated  $\Delta G_{CS}^0$  and  $\Delta G_{CR}^0$  are listed in Table 2.

**Steady-State Absorption Studies.** Figure 4 shows steady-state absorption spectra of C<sub>60</sub>-(BTD-TPA), NMPC<sub>60</sub> and BTD-TPA in toluene. The absorption band of C<sub>60</sub>-(BTD-TPA) at 440 nm is mainly attributed to charge-transfer (CT) transition within

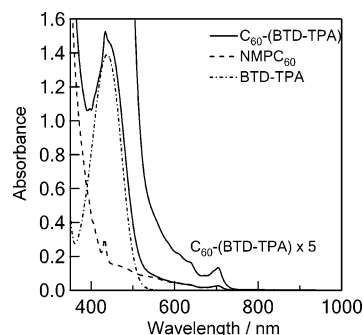


**Figure 4.** Steady-state absorption spectra of C<sub>60</sub>-(BTD-TPA) (0.02 mM), NMPC<sub>60</sub> (0.02 mM), and BTD-TPA (0.02 mM) in toluene.

the BTD-TPA moiety, because they act as acceptor and donor, respectively.<sup>21</sup> The absorption bands of the C<sub>60</sub> moiety appeared at both 705 nm and below 350 nm.<sup>30</sup> No additional absorption band or no appreciable shift were observed for C<sub>60</sub>-(BTD-TPA)

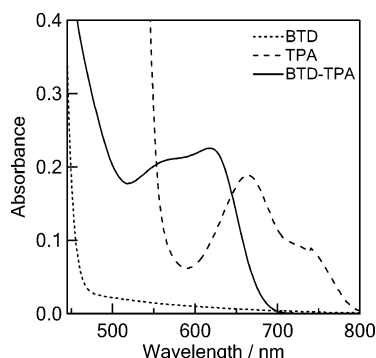


**Figure 5.** Steady-state absorption spectra of BTD (0.1 mM), TPA (0.1 mM), and BTD-TPA (0.1 mM) in the presence of  $\text{FeCl}_3$  in PhCN.

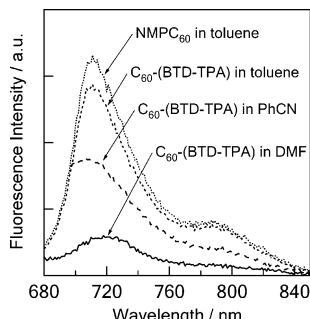


**Figure 6.** Steady-state fluorescence spectra of  $\text{C}_{60}$ -(BTD-TPA) and  $\text{NMP-C}_{60}$  (0.1 mM) in DMF, PhCN and toluene;  $\lambda_{\text{ex}} = 600$  nm.

compared with the sum of the absorptions of  $\text{NMPC}_{60}$  and BTD-TPA. This finding suggests that there is no strong interaction in the ground state between the  $\text{C}_{60}$  and BTD-TPA moieties. Similar results were obtained in PhCN and DMF. In the transient absorption measurements in the present study, the selective excitation of the  $\text{C}_{60}$  moiety in  $\text{C}_{60}$ -(BTD-TPA) was possible with 532 nm laser light, since BTD-TPA has not considerable absorbance at this wavelength. By the excitation at 440 nm, 90% of the BTD-TPA moiety and 10% of the  $\text{C}_{60}$  moiety can be excited.

On addition of  $\text{FeCl}_3$  to TPA and BTD-TPA in PhCN, new absorption bands appeared in the visible region as shown in Figure 5, whereas no extra absorption was observed for BTD, resisting against oxidation by  $\text{FeCl}_3$ . A broad absorption band appeared at 665 nm for TPA with shoulder at 740 nm can be attributed to  $\text{TPA}^{\bullet+}$ . The main peak is in agreement with the reported absorption bands of the radical cation of unsubstituted TPA, exhibiting its absorption around 650 nm.<sup>31</sup> In the case of BTD-TPA, the absorption band shifted to 640 nm, suggesting that the radical cation delocalizes on the BTD-TPA moiety. This is in good agreement with the HOMO in Figure 2. The extinction coefficient ( $\epsilon_{640\text{nm}}$ ) of the absorption peak of  $(\text{BTD-TPA})^{\bullet+}$  was evaluated as about  $10000 \text{ M}^{-1} \text{ cm}^{-1}$ .

**Steady-State Fluorescence Studies.** Figure 6 shows the steady-state fluorescence spectra of  $\text{C}_{60}$ -(BTD-TPA) measured with the excitation at 600 nm in toluene, PhCN, and DMF. The fluorescence peak at 710 nm is attributed to that of the  $\text{C}_{60}$  moiety in  $\text{C}_{60}$ -(BTD-TPA) being referred to the fluorescence peak of  $\text{NMPC}_{60}$ .<sup>30</sup> By comparing the fluorescence peak and absorption peak (705 nm), it was revealed that  $^1\text{C}_{60}^*-(\text{BTD-TPA})$  shows small Stokes shift and has the lowest singlet excited energy at 1.75 eV.<sup>30</sup> The fluorescence intensity of  $^1\text{C}_{60}^*-(\text{BTD-TPA})$  in toluene was almost the same as that of  $\text{NMPC}_{60}$ , while the fluorescence intensities of  $^1\text{C}_{60}^*-(\text{BTD-TPA})$  decrease with solvent polarity; that is, the peak intensity decreased by factors of 1/2 in PhCN and 1/5 in DMF, comparing with that in toluene.

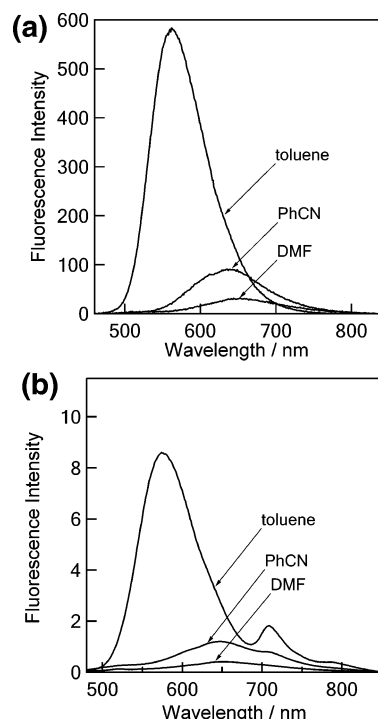


**Figure 7.** Steady-state fluorescence spectra of (a) BTD-TPA and (b)  $\text{C}_{60}$ -(BTD-TPA) (0.1 mM) in DMF, PhCN, and toluene;  $\lambda_{\text{ex}} = 450$  nm.

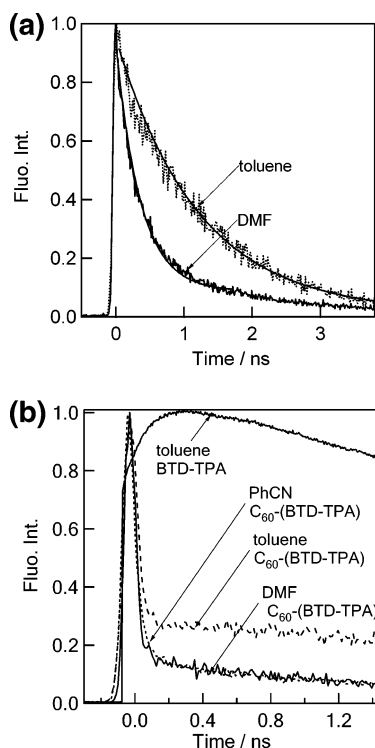
These observations suggest that the CS process predominantly takes place from  $^1\text{C}_{60}^*-(\text{BTD-TPA})$ , generating  $\text{C}_{60}^{\bullet-}-(\text{BTD-TPA})^{\bullet+}$  by the excitation with 600 nm light.

Figure 7a shows steady-state fluorescence spectra of BTD-TPA in toluene, PhCN, and DMF with excitation at 450 nm, which selectively excites the CT absorption band of the BTD-TPA moiety. In toluene, the fluorescence peak appeared at 555 nm. By comparing the fluorescence peak with the absorption peak (440 nm), it was revealed that BTD-TPA shows appreciable Stokes shift ( $4700 \text{ cm}^{-1}$ ) and has the lowest singlet excited energy at 2.23 eV in toluene.<sup>32</sup> In PhCN and DMF, fluorescence peaks shifted to 640 and 655 nm, respectively, with decreasing the fluorescence intensities. Such large shifts of the emission spectra to longer wavelengths in polar solvents can be explained by stabilization of the excited singlet state of BTD-TPA by polar solvents.<sup>21</sup> The energy levels of the stabilized singlet excited state were estimated to be 1.94 and 1.89 eV in PhCN and DMF, respectively.<sup>32</sup> The decrease in the emission intensities in polar solvents can be attributed to the excited CT complex formation between the BTD and TPA moieties.<sup>21,33</sup>

Compared with the fluorescence intensity of BTD-TPA at 555 nm in toluene, the fluorescence intensity of the BTD-TPA moiety in  $\text{C}_{60}$ -(BTD-TPA) at 575 nm (Figure 7b) decreased very much even in nonpolar toluene by a factor of ca. 1/50 (Supporting Information, Figure S1a), suggesting the intramolecular energy transfer (EN) from  $\text{C}_{60}^1-(\text{BTD-TPA})^*$  to  $^1\text{C}_{60}^*-(\text{BTD-TPA})$ , which can be confirmed by the appearance of the fluorescence peak at 715 nm in Figure 7b.<sup>30</sup> In polar solvents, further decrease in the fluorescence intensity were observed by the comparison of part b in Figure 7 with part a, which suggests that the CS process occurs in addition to the EN process, generating  $\text{C}_{60}^{\bullet-}-(\text{BTD-TPA})^{\bullet+}$  and  $^1\text{C}_{60}^*-(\text{BTD-TPA})$ , respectively.

For  $\text{C}_{60}$ -BTD, only 710 nm fluorescence peak due to the  $^1\text{C}_{60}^*$  moiety was observed in toluene, PhCN, and DMF by the selective excitation of  $\text{C}_{60}$  (Supporting Information, Figure S1b). However, the fluorescence intensity of  $^1\text{C}_{60}^*$ -BTD did not





**Figure 8.** Fluorescence decays of C<sub>60</sub>-(BTD-TPA) with excitation at 410 nm and detection at (a) 710 nm and (b) 555 nm in toluene and 640 nm in PhCN and DMF.

change appreciably with a change in the solvent polarity, indicating no CS process via the <sup>1</sup>C<sub>60</sub>\* moiety. By the excitation of the BTD moiety in C<sub>60</sub>-BTD, the fluorescence intensities at 550–600 nm decreased considerably compared to that of BTD as shown in Supporting Information (Figure S1c), suggesting that appreciable EN process generating <sup>1</sup>C<sub>60</sub>\*-BTD from C<sub>60</sub>-<sup>1</sup>BTD\* is present. These observations indicate that the BTD moiety acts as a unique antenna molecule, only when the TPA and C<sub>60</sub> moieties are connected in the both sides.

**Fluorescence Lifetime Measurements.** The fluorescence lifetimes (τ<sub>f</sub>) of C<sub>60</sub>-(BTD-TPA) and BTD-TPA were measured using a time-correlated single-photon-counting apparatus with excitation at 410 nm as shown in Figure 8a. In toluene, the fluorescence time profile of <sup>1</sup>C<sub>60</sub>\*-(BTD-TPA) at 710 nm shows single-exponential decay, giving the τ<sub>f</sub> value of 1480 ps, which is nearly equal to that of NMPC<sub>60</sub> (1300 ps).<sup>34</sup> In PhCN, the τ<sub>f</sub> value of <sup>1</sup>C<sub>60</sub>\*-BTD-TPA was evaluated to be 570 ps by a single-exponential decay. In DMF, the time profile shows biexponential decay; a major contribution (85%) was the fast decay component (290 ps) and the slow decay component (ca. 1400 ps) with minor contribution (15%).<sup>35</sup> From these τ<sub>f</sub> values, the rate constant (k<sub>CS</sub><sup>I</sup>) and the quantum yield (Φ<sub>CS</sub><sup>I</sup>) for the CS processes via <sup>1</sup>C<sub>60</sub>\*-(BTD-TPA) were calculated by eqs 3 and 4, where the (τ<sub>f</sub>)<sub>sample</sub> and (τ<sub>f</sub>)<sub>ref</sub> refer to the fluorescence lifetimes of sample and reference, respectively<sup>8–13</sup>

$$k_{CS}^I = (1/\tau_{f, \text{sample}} - 1/\tau_{f, \text{ref}}) \quad (3)$$

$$\Phi_{CS}^I = [(1/\tau_{f, \text{sample}} - 1/\tau_{f, \text{ref}}) / (1/\tau_{f, \text{sample}})] \quad (4)$$

These values are listed in Table 2.

Figure 8b shows the fluorescence time profiles of C<sub>60</sub>-<sup>1</sup>(BTD-TPA)\* at 555 nm in toluene and 640 nm in PhCN and DMF. In all solvents, the time profiles show two component decay; major components decay very quick with the τ<sub>f</sub> value of 30–

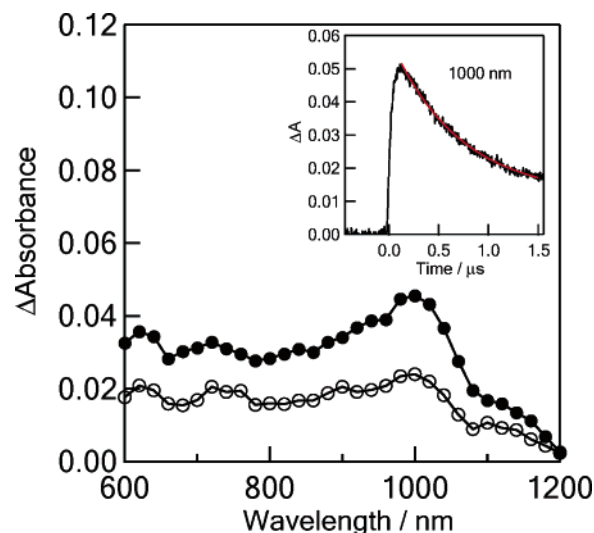


**Figure 9.** Nanosecond transient absorption spectra of C<sub>60</sub>-(BTD-TPA)- (0.1 mM) at 0.1 μs (●) and 1.0 μs (○) after 532 nm laser irradiation. Inset: Absorption–time profiles at 1000 nm in DMF.

50 ps, while minor slow decay components gave the τ<sub>f</sub> value of 4800–5000 ps. In toluene, the shorter τ<sub>f</sub> value (50 ps) was assigned to the EN process from C<sub>60</sub>-<sup>1</sup>(BTD-TPA)\* to <sup>1</sup>C<sub>60</sub>\*-(BTD-TPA); thus, the k<sub>EN</sub> and Φ<sub>EN</sub> values can be evaluated from the same equations as eqs 3 and 4 using the lifetime of BTD-TPA as a standard.<sup>36</sup> In polar solvents, the τ<sub>f</sub> values become further short to 30 ps. Since the solvent polarity effect on the k<sub>EN</sub> values may be small, we can assume the same k<sub>EN</sub> values for all solvents. Thus, the direct CS process from C<sub>60</sub>-<sup>1</sup>(BTD-TPA)\* to C<sub>60</sub>\*-(BTD-TPA)<sup>•+</sup>, which refer to the k<sub>CS</sub><sup>II</sup> and Φ<sub>CS</sub><sup>II</sup> values, can be evaluated by eqs 5 and 6

$$k_{CS}^{II} = (1/\tau_{f, \text{dyad, polar-solvent}} - 1/\tau_{f, \text{dyad, non-polar-solvent}}) \quad (5)$$

$$\Phi_{CS}^{II} = k_{CS}^{II} / (1/\tau_{f, \text{dyad, polar-solvent}}) \quad (6)$$

These values are also listed in Table 2. From the negative ΔG<sub>CS</sub> values in polar solvents, the CS processes via the <sup>1</sup>C<sub>60</sub>\* and <sup>1</sup>(BTD-TPA)\* moieties in C<sub>60</sub>-BTD-TPA are thermodynamically favorable; thus, k<sub>CS</sub><sup>I</sup> and k<sub>CS</sub><sup>II</sup> can be attributed to the CS process via the <sup>1</sup>C<sub>60</sub>\* and <sup>1</sup>(BTD-TPA)\* moieties in C<sub>60</sub>-(BTD-TPA), respectively.

**Time-Resolved Transient Absorption Spectra.** A transient absorption spectrum of C<sub>60</sub>-(BTD-TPA) observed in toluene by nanosecond laser light excitation at 532 nm showed a peak at 700 nm, which was attributed to the <sup>3</sup>C<sub>60</sub>\* moiety in C<sub>60</sub>-BTD-TPA.<sup>34</sup> In the transient spectrum of C<sub>60</sub>-(BTD-TPA) in DMF (Figure 9), on the other hand, the transient absorption bands appeared around 1000 nm, which is attributed to the C<sub>60</sub>\*- moiety.<sup>30</sup> The broad absorption bands in the visible region around 620 and 720 nm were assigned to that of the (BTD-TPA)\*<sup>•+</sup> moiety in C<sub>60</sub>-(BTD-TPA) as shown in Figure 5. Thus, generation of the CS state (C<sub>60</sub>\*-(BTD-TPA)<sup>•+</sup>) via <sup>1</sup>C<sub>60</sub>\*-(BTD-TPA) can be confirmed. From the comparison with the concentration of <sup>3</sup>C<sub>60</sub>\* moiety generated on laser light pulse, the quantum yield of generation of C<sub>60</sub>\*-(BTD-TPA)<sup>•+</sup> was evaluated from the transient spectra to be 0.76 (Supporting Information, Figure S2), which is almost the same as evaluated from the fluorescence lifetimes (0.81).

In PhCN (Supporting Information, Figure S3), absorption bands due to the CS state was not appreciable in the initial time, since the absorption bands of C<sub>60</sub>\*-(BTD-TPA)<sup>•+</sup> are hidden by the intense absorption of <sup>3</sup>C<sub>60</sub>\*-BTD-TPA. However, the



takes place, resulting in the observation of the absorption of <sup>3</sup>C<sub>60</sub>\* with long lifetime than 20 μs.<sup>30</sup> In polar solvents, the CS process via <sup>1</sup>C<sub>60</sub>\* is possible. In DMF, the CS process via <sup>3</sup>C<sub>60</sub>\* is also possible, which may be related to the long lifetime of C<sub>60</sub>\*-(BTD-TPA)<sup>•+</sup>, because C<sub>60</sub>\*-(BTD-TPA)<sup>•+</sup> gains the triplet spin character, when the precursor is <sup>3</sup>C<sub>60</sub>\*-(BTD-TPA).<sup>9c,18</sup>

Short lifetimes of C<sub>60</sub>-<sup>1</sup>(BTD-TPA)\* in nopolarsolvents suggest that the EN process predominantly takes place. In polar solvents, the direct CS process takes place generating C<sub>60</sub>\*-(BTD-TPA)<sup>•+</sup> in addition to the EN process generating <sup>1</sup>C<sub>60</sub>\*-(BTD-TPA), which is finally converted to C<sub>60</sub>\*-(BTD-TPA)<sup>•+</sup>. These ultimate C<sub>60</sub>\*-(BTD-TPA)<sup>•+</sup> are persistent due to the small reorganization energy characteristic of the fullerene derivatives.

**Comparison with Other Dyads and Triads.** Since C<sub>60</sub>-(BTD-TPA) has two routes for CS processes, the lights in the wide wavelength region can be utilized for the CS processes. In the direct CS process from <sup>1</sup>C<sub>60</sub>\*-BTD-TPA to C<sub>60</sub>\*-(BTD-TPA)<sup>•+</sup>, the BTD-TPA moiety acts as a good electron donor. In the indirect CS process generating C<sub>60</sub>\*-(BTD-TPA)<sup>•+</sup> via <sup>1</sup>C<sub>60</sub>\*-BTD-TPA after the EN process from C<sub>60</sub>-<sup>1</sup>(BTD-TPA)\*, the BTD-TPA moiety acts as antenna, too. In the ultimate CS state (C<sub>60</sub>\*-(BTD-TPA)<sup>•+</sup>), the BTD moiety also has a role to stabilize the TPA<sup>•+</sup> moiety as a substituent.

In the CR process, the τ<sub>RIP</sub> value in DMF at room temperature was evaluated to be 690 ns, which is longer than the reported τ<sub>RIP</sub> value for the C<sub>60</sub> dyads with aromatic amines. For example, the τ<sub>RIP</sub> value of C<sub>60</sub>-TPA dyad was less than 10 ns.<sup>39</sup> The τ<sub>RIP</sub> value for a dyad composed of the C<sub>60</sub>-(fluorene-diphenylamine) was evaluated to be 150 ns in DMF at room temperature.<sup>18</sup> In the case of C<sub>60</sub>-bridge-dimethylaniline systems, the τ<sub>RIP</sub> values in the range of 8–250 ns were reported, depending on the kinds and lengths of the bridge molecules.<sup>10a,b</sup> When these C<sub>60</sub> and amine dyads are compared, C<sub>60</sub>\*-(BTD-TPA)<sup>•+</sup> showed long τ<sub>RIP</sub> value among the C<sub>60</sub> connected with aromatic amine systems using various bridges in solutions. In other systems of porphyrins connected with C<sub>60</sub> and chlorins connected with C<sub>60</sub> systems, longer lifetimes were recently reported in low-temperature rigid media.<sup>40</sup> Therefore, there remains to design other aromatic-amine connected C<sub>60</sub> systems based on the data described in these studies.

## Conclusions

For [60]fullerene covalently linked to BTD-TPA, photoinduced CS and EN processes takes place via both <sup>1</sup>C<sub>60</sub>\* and <sup>1</sup>(BTD-TPA)\* moieties producing ultimate CS state (C<sub>60</sub>\*-(BTD-TPA)<sup>•+</sup>) in polar solvent. In the initial step, the coupled BTD-TPA moiety acts as a good light-harvesting antenna and an efficient energy-transfer reagent to the C<sub>60</sub> moiety. In the electron-transfer step, the BTD-TPA moiety acts as an electron donor. The BTD-TPA moiety increases the efficiency of the CS process and prolongs the lifetime of the CR process. The origins of such effects of the BTD-TPA moiety of C<sub>60</sub>-BTD-TPA, which can be thought as coupled donor system, were revealed by the time-resolved measurements. Prolong lifetime of C<sub>60</sub>\*-(BTD-TPA)<sup>•+</sup> in DMF can be interpreted by the Marcus inverted region on the basis of the reorganization energy experimentally evaluated by the temperature dependence of the rate constants.

Furthermore, the present study provides a new possibility of the benzothiadiazole functional dyes, which can be developed newly to light-harvesting as well as donor functionality in photovoltaic, in addition to other functional materials such as

light-emitting materials in OLEDs,<sup>21</sup> dichroic fluorescent materials in liquid crystal displays,<sup>23</sup> and red-fluorescent two-photon-absorbing materials in laser scanning fluorescence imaging.<sup>24</sup> We believe that the present study gives us valuable information not only in the photoinduced electron-transfer chemistry of fullerene-dyad systems but also in the materials science of benzothiadiazole-based functional dyes.

## Experimental Section

**General.** All melting points are uncorrected. IR spectra were recorded on a JASCO FT/IR-470 plus Fourier transform infrared spectrometer and measured as KBr pellets or Nujol. <sup>1</sup>H NMR spectra were determined in CDCl<sub>3</sub> or CDCl<sub>3</sub>/CS<sub>2</sub> with a JEOL EX-270 spectrometer. Residual solvent protons were used as internal standard and chemical shifts (δ) are given relative to tetramethylsilane (TMS). The coupling constants (*J*) were reported in Hz. Elemental analysis was performed at the Elemental Analytical Center, Kyushu University. EI-MS spectra were recorded with a JEOL JMS-70 mass spectrometer at 70 eV using a direct inlet system. FAB-MS was recorded with a JEOL JMS-70 mass spectrometer with *m*-nitrobenzyl alcohol (NBA) as a matrix. Gel permeation chromatography (GPC) was performed with a Japan Analytical Industry Co., Ltd LC-908 using JAIGEL-1H column (20 × 600 mm) and JAIGEL-2H column (20 × 600 mm) eluting with chloroform (3.0 mL/min). Analytical TLC was carried out on silica gel coated on aluminum foil (Merck 60 F<sub>254</sub>). Column chromatography was carried out on silica gel (Wako C-300). Compounds NMPC<sub>60</sub>,<sup>27</sup> BTD,<sup>20a</sup> and **1**<sup>41</sup> were prepared according to methods reported previously.

**4-Bromo-7-[4-(diphenylamino)phenyl]-2,1,3-benzothiadiazole (2a).** To a mixture of **1** (1.00 g, 3.40 mmol) in benzene (32 mL) and aqueous 2 M sodium carbonate solution (21 mL) was added 4-diphenylaminophenylboronic acid (983 mg, 3.40 mmol) in ethanol (20 mL) under an argon atmosphere. Subsequently, tetrakis(triphenylphosphine)palladium (0) (118 mg, 0.102 mmol) was added to the mixture at 60 °C. After the mixture was heated at 80 °C for 15 h, the reaction mixture was poured into water and extracted with chloroform. The organic layer was dried over anhydrous magnesium sulfate and evaporated in vacuo to dryness. The residue was separated by column chromatography on silica gel (dichloromethane/*n*-hexane, 1:1 (v/v)) to give crude **2a** (purity of 80 mol-%, 1.39 g) containing 4,7-bis[4-(diphenylamino)phenyl]-2,1,3-benzothiadiazole as an orange powder. The inseparable mixture was used to next reaction. <sup>1</sup>H NMR (CDCl<sub>3</sub>) δ 7.08 (t, *J* = 7.3 Hz, 2 H, *p*-phenyl-H), 7.16–7.33 (m, 10 H, phenyl-H and phenylene-H), 7.55 (d, *J* = 7.3 Hz, 1 H, ArH), 7.81 (d, *J* = 8.9 Hz, 2 H, phenylene-H), 7.90 (d, *J* = 7.3 Hz, 1 H, ArH).

**4-Bromo-7-phenyl-2,1,3-benzothiadiazole (2b).** According to a method similar to the preparation of **2a**, **2b** was obtained as a mixture containing 4,7-diphenyl-2,1,3-benzothiadiazole (purity of 78 mol-%, 5.42 g) from benzene (190 mL), aqueous 2 M sodium carbonate solution (122 mL), phenylboronic acid (2.74 g, 22.5 mmol), ethanol (65 mL), and tetrakis(triphenylphosphine)palladium (0) (707 mg, 0.612 mmol). The crude product was purified by column chromatography on silica gel (dichloromethane/*n*-hexane, 3:2 (v/v)) and by recrystallization (ethanol/chloroform). The inseparable mixture was used in the next reaction. Yellow needles; <sup>1</sup>H NMR (CDCl<sub>3</sub>) δ 7.50 (t, *J* = 7.3 Hz, 1 H, *p*-phenyl-H), 7.54 (t, *J* = 7.6 Hz, 2 H, *m*-phenyl-H), 7.87, 7.89 (d, *J* = 7.9 Hz, each 1 H, ArH), 7.94 (d, *J* = 7.6 Hz, 2 H, *o*-phenyl-H).

**4-[4-(Diphenylamino)phenyl]-7-(4-formylphenyl)-2,1,3-benzothiadiazole (3a).** According to a method similar to the



preparation of **2a**, **3a** was obtained in 82% yield (347 mg, 0.719 mmol) from crude **2a** (80 mol-% purity, 500 mg, 0.872 mmol), benzene (11 mL), aqueous 2 M sodium carbonate solution (7 mL), 4-formylphenylboronic acid (180 mg, 1.20 mmol), ethanol (11 mL), and tetrakis(triphenylphosphine)palladium (0) (37.8 mg, 0.0327 mmol). The crude product was purified by column chromatography on silica gel (dichloromethane/*n*-hexane, 1:1 (v/v)) and by GPC (chloroform). Reddish orange powder; mp 200–201 °C; IR (Nujol mull,  $\text{cm}^{-1}$ ) 1695 ( $\nu_{\text{C=O}}$ ), 1591, 1277, 1173, 822, 723, 695;  $^1\text{H}$  NMR ( $\text{CDCl}_3$ )  $\delta$  7.08 (t,  $J = 7.3$  Hz, 2 H, *p*-phenyl-H), 7.18–7.34 (m, 10 H, phenyl-H and phenylene-H), 7.79, 7.86 (d,  $J = 7.6$  Hz, each 1 H, ArH), 7.90 (d,  $J = 8.9$  Hz, 2 H, phenylene-H), 8.05, 8.17 (d,  $J = 8.3$  Hz, each 2 H, phenylene-H), 10.12 (s, 1 H, CHO); EI-MS (positive)  $m/z$  483 ( $\text{M}^+$ ). Anal. Calcd for  $\text{C}_{31}\text{H}_{21}\text{N}_3\text{OS}\cdot 0.2\text{CHCl}_3$ : C, 75.91; H, 4.41; N, 8.51. Found: C, 75.96; H, 4.36; N, 8.50.

**4-(4-Formylphenyl)-7-phenyl-2,1,3-benzothiadiazole (3b).** According to a method similar to the preparation of **2a**, **3b** was obtained in 84% yield (712 mg, 2.25 mmol) from crude **2b** (78 mol-% purity, 1.00 g, 2.68 mmol), benzene (32 mL), aqueous 2 M sodium carbonate solution (21 mL), 4-formylphenylboronic acid (565 mg, 3.77 mmol), ethanol (16 mL), and tetrakis(triphenylphosphine)palladium (0) (119 mg, 0.103 mmol). The crude product was purified by column chromatography on silica gel (dichloromethane/*n*-hexane, 3:2 (v/v)). Yellow needles; mp 328–330 °C; IR (Nujol mull,  $\text{cm}^{-1}$ ) 1697 ( $\nu_{\text{C=O}}$ ), 1603, 1544, 1510, 1492, 1476, 1447, 1306, 1212, 1167, 1105, 1074, 828, 798, 758, 694;  $^1\text{H}$  NMR ( $\text{CDCl}_3$ )  $\delta$  7.49 (t,  $J = 7.9$  Hz, 1 H, *p*-phenyl-H), 7.57 (t,  $J = 7.9$  Hz, 2 H, *m*-phenyl-H), 7.83, 7.89 (d,  $J = 7.6$  Hz, each 1 H, ArH), 7.98 (d,  $J = 7.9$  Hz, 2 H, *o*-phenyl-H), 8.07, 8.18 (d,  $J = 8.3$  Hz, each 2 H, phenylene-H), 10.13 (s, 1 H, CHO); EI-MS (positive)  $m/z$  316 ( $\text{M}^+$ ). Anal. Calcd for  $\text{C}_{19}\text{H}_{12}\text{N}_2\text{OS}$ : C, 72.13; H, 3.82; N, 8.85. Found: C, 71.98; H, 3.87; N, 8.87.

**4-[4-(Diphenylamino)phenyl]-7-(4-tolyl)-2,1,3-benzothiadiazole (BTD-TPA).** According to a method similar to the preparation of **2a**, BTD-TPA was obtained in 61% yield (50 mg, 0.106 mmol) from crude **2a** (80 mol-% purity, 100 mg, 0.174 mmol), benzene (5 mL), aqueous 2 M sodium carbonate solution (3 mL), 4-tolylboronic acid (32.6 mg, 0.240 mmol), ethanol (3 mL), and tetrakis(triphenylphosphine)palladium (0) (7.6 mg, 0.0065 mmol). The crude product was purified by column chromatography on silica gel (dichloromethane/*n*-hexane, 2:3 (v/v)) and by GPC (chloroform). Yellowish orange powder: mp 192–194 °C; IR (Nujol mull,  $\text{cm}^{-1}$ ) 1589, 1316, 1279, 1186, 888, 817, 745, 698;  $^1\text{H}$  NMR ( $\text{CDCl}_3$ )  $\delta$  2.45 (s, 3 H,  $\text{CH}_3$ ), 7.07 (t,  $J = 7.2$  Hz, 2 H, *p*-phenyl-H), 7.17–7.37 (m, 12 H, phenyl-H and phenylene-H), 7.75 (s, 2 H, ArH), 7.86, 7.88 (d,  $J = 8.6$  Hz, each 2 H, phenylene-H); FAB-MS (positive)  $m/z$  469 ( $\text{M}^+$ ). Anal. Calcd for  $\text{C}_{31}\text{H}_{23}\text{N}_3\text{S}$ : C, 79.29; H, 4.94; N, 8.95. Found: C, 78.92; H, 5.00; N, 8.87.

**[60]Fullerene-2,1,3-benzothiadiazole-triphenylamine dyad (C<sub>60</sub>-(BTD-TPA)).** A solution of [60]fullerene (149 mg, 0.208 mmol), *N*-methyl glycine (22 mg, 0.248 mmol), and **3a** (100 mg, 0.207 mmol) in *p*-xylene (50 mL) was heated at the refluxing temperature for 19 h under an argon atmosphere. After the solvent was removed in vacuo, the residue was purified by column chromatography on silica gel (toluene/*n*-hexane, 4:1 (v/v)) to give C<sub>60</sub>-BTD-TPA in 16% yield (40 mg, 0.033 mmol) as a brown solid: mp >450 °C; IR (KBr,  $\text{cm}^{-1}$ ) 2949, 2919, 2854, 1591, 1487, 1332, 1281, 1179, 888, 824, 752, 696, 526;  $^1\text{H}$  NMR ( $\text{CDCl}_3/\text{CS}_2$ , 8:1 (v/v))  $\delta$  2.87 (s, 3 H,  $\text{N}-\text{CH}_3$ ), 4.31, 5.02 (d,  $J = 9.2$  Hz, each 1 H, methylene-H), 5.03 (s, 1 H, methyne-H), 7.05 (t,  $J = 7.3$  Hz, 2 H, *p*-phenyl-H), 7.15–7.38

(m, 10 H, phenyl-H and phenylene-H), 7.73, 7.82 (d,  $J = 7.6$  Hz, each 1 H, ArH), 7.87 (d,  $J = 8.9$  Hz, 2 H, phenylene-H), 7.95, 8.10 (d,  $J = 7.3$  Hz, each 2 H, phenylene-H); FAB-MS (NBA, positive)  $m/z$  1231 ( $\text{M}^+$ ). Anal. Calcd for  $\text{C}_{93}\text{H}_{26}\text{N}_4\text{S}\cdot 0.5\text{C}_7\text{H}_8$ : C, 90.73; H, 2.37; N, 4.39. Found: C, 90.37; H, 2.60; N, 4.36.

**[60]Fullerene-2,1,3-benzothiadiazole Dyad (C<sub>60</sub>-BTD).** According to a method similar to the preparation of C<sub>60</sub>-BTD-TPA, C<sub>60</sub>-BTD was obtained in 23% yield (79 mg, 0.0742 mmol) from [60]fullerene (231 mg, 0.32 mmol), *N*-methyl glycine (34 mg, 0.38 mmol), **3b** (100 mg, 0.32 mmol), and *p*-xylene (50 mL). The crude product was purified by column chromatography on silica gel (toluene/*n*-hexane, 4:1 (v/v)). Brown solid; mp >450 °C; IR (KBr,  $\text{cm}^{-1}$ ) 2946, 2777, 1333, 1260, 1180, 1107, 887, 834, 758, 693, 526;  $^1\text{H}$  NMR ( $\text{CDCl}_3/\text{CS}_2=7:1$ )  $\delta$  2.88 (s, 3 H,  $\text{N}-\text{CH}_3$ ), 4.31, 5.03 (d,  $J = 9.6$  Hz, each 1 H,  $\text{CH}_2$ ), 5.04 (s, 1 H, CH), 7.44 (t,  $J = 7.6$  Hz, 1 H, *p*-phenyl-H), 7.54 (t,  $J = 7.6$  Hz, 2 H, *m*-phenyl-H), 7.77, 7.84 (d,  $J = 7.6$  Hz, each 1 H, ArH), 7.94 (d,  $J = 7.6$  Hz, 2 H, *o*-phenyl-H), 7.98 (d,  $J = 8.6$  Hz, 2 H, phenylene-H), 8.10 (d,  $J = 8.6$  Hz, 2 H, phenylene); FAB-MS (NBA, negative)  $m/z$  1064 ( $\text{M}^-$ ), 720 ( $\text{C}_{60}^-$ ). Anal. Calcd for  $\text{C}_{81}\text{H}_{17}\text{N}_3\text{S}\cdot 0.5\text{C}_7\text{H}_8$ : C, 90.83; H, 2.26; N, 3.92. Found: C, 90.73; H, 2.01; N, 3.65.

**Spectral Measurements.** Time-resolved fluorescence spectra were measured by a single-photon counting method using a second harmonic generation (SHG, 410 nm) of a Ti:sapphire laser [Spectra Physics, Tsunami 3950-L2S, 1.5 ps full width at half-maximum (fwhm)] and a streak scope (Hamamatsu Photonics, C4334-01) equipped with a polychromator (Action Research, SpectraPro 150) as an excitation source and a detector, respectively.<sup>42</sup>

Nanosecond transient absorption measurements were carried out using SHG (532 nm) of Nd:YAG laser (Spectra Physics, Quanta-Ray GCR-130, fwhm 6 ns) as an excitation source. For transient absorption spectra in the near-IR region (600–1600 nm), monitoring light from a pulsed Xe lamp was detected with a Ge-avalanche photodiode (Hamamatsu Photonics, B2834). Photoinduced events in micro- and millisecond time regions were estimated by using a continuous Xe lamp (150 W) and an InGaAs-PIN photodiode (Hamamatsu Photonics, G5125-10) as a probe light and a detector, respectively. Details of the transient absorption measurements were described elsewhere.<sup>43</sup> All the samples in a quartz cell (1 × 1 cm) were deaerated by bubbling argon through the solution for 15 min. Steady-state absorption spectra in the visible and near-IR regions were measured on a JASCO V570 DS spectrometer. Fluorescence spectra were measured on a Shimadzu RF-5300PC spectrofluorophotometer.

**Electrochemical Measurements.** The cyclic voltammetry measurements were performed on a BAS CV-50 W electrochemical analyzer in deaerated PhCN or DMF solution (0.1 mM) containing 0.1 M tetra-*n*-butylammonium perchlorate as a supporting electrolyte at 298 K (100 mV s<sup>-1</sup>). The glassy carbon working electrode was polished with BAS polishing alumina suspension and rinsed with acetone before use. The counter electrode was a platinum wire. The measured potentials were recorded with respect to an Ag/AgCl (saturated KCl) reference electrode and  $\text{Fc}/\text{Fc}^+$  was used as an internal standard.

**Theoretical Calculations.** All calculations were performed by semiempirical PM3 and density function B3LYP/3-21G(\*) method with Gaussian 98 package.<sup>28</sup> The graphics of HOMO and LUMO coefficients were generated with the help of Gauss View software.



**Acknowledgment.** The present work was partly supported by a Grant-in-Aid for Scientific Research on Primary Area (417) from the Ministry of Education, Science, Sports and Culture of Japan.

**Supporting Information Available:** Fluorescence lifetimes of BTD-TPA. Steady-state fluorescence spectra of BTD-TPA and C<sub>60</sub>-(BTD-TPA). Nanosecond transient absorption spectra of C<sub>60</sub>-(BTD-TPA) and C<sub>60</sub>-BTD. Evaluation of the quantum yield of the generation of charge-separated state by the transient absorption spectra. Long-time measurement of time profile at 1000 nm of C<sub>60</sub>-(BTD-TPA) in PhCN. Temperature-dependent absorbance profiles at 1000 nm of C<sub>60</sub>-(BTD-TPA) in DMF. The IR spectra of BTD-TPA and C<sub>60</sub>-(BTD-TPA). This material is available free of charge via the Internet at <http://pubs.acs.org>.

## References and Notes

- (1) Foote, C. S. In *Topics in Current Chemistry; Photophysical and Photochemical Properties of Fullerenes*; Matty, J., Ed.; Springer-Verlag: Berlin, 1994; Series 169, p 347.
- (2) *Fullerene, Chemistry, Physics and Technology*; Kadish, K. M., Ruoff, R. S., Eds.; Wiley-Interscience: New York, 2000.
- (3) *Molecular and Supramolecular Photochemistry*; Ramamurthy, V., Schanze, K. S., Eds.; Marcel Dekker: New York, 2001; Vol. 7.
- (4) (a) Imahori, H.; Sakata, Y. *Adv. Mater.* **1997**, *9*, 537. (b) Martín, N.; Sánchez, L.; Illescas, B.; Pérez, I. *Chem. Rev.* **1998**, *98*, 2527. (c) Guldi, D. M.; Prato, M. *Acc. Chem. Res.* **2000**, *33*, 695.
- (5) Echegoyen, L.; Echegoyen, L. E. *Acc. Chem. Res.* **1998**, *31*, 593.
- (6) Gust, D.; Moore, T. A.; Moore, A. L. *Acc. Chem. Res.* **2001**, *34*, 40.
- (7) (a) Imahori, H.; Hagiwara, K.; Akiyama, T.; Akoi, M.; Taniguchi, S.; Okada, T.; Shirakawa, M.; Sakata, Y. *Chem. Phys. Lett.* **1996**, *263*, 545. (b) Guldi, D. M.; Asmus, K.-D. *J. Am. Chem. Soc.* **1997**, *119*, 5744. (c) Imahori, H.; El-Khouly, M. E.; Fujitsuka, M.; Ito, O.; Sakata, Y.; Fukuzumi, S. *J. Phys. Chem. A* **2001**, *105*, 325. (d) Imahori, H.; Tamaki, K.; Guldi, D. M.; Luo, C.; Fujitsuka, M.; Ito, O.; Sakata, Y.; Fukuzumi, S. *J. Am. Chem. Soc.* **2001**, *123*, 2607. (e) Vehmanen, V.; Tkachenko, N. V.; Imahori, H.; Fukuzumi, S.; Lemmetyinen, H. *Spectrochim. Acta, Part A* **2001**, *57*, 2229.
- (8) (a) *The Photosynthetic Reaction Center*; Deisenhofer, J., Norris, J. R., Eds.; Academic Press: San Diego, CA, 1993. (b) *Anoxygenic Photosynthetic Bacteria*; Blankenship, R. E., Madigan, M. T., Bauer, C. E., Eds.; Kluwer Academic Publishing: Dordrecht, The Netherlands, 1995. (c) Wasielewski, M. R.; Wiederrecht, G. P.; Svec, W. A.; Niemczyk, M. P. *Sol. Energy Mater. Solar Cells* **1995**, *38*, 127.
- (9) (a) Imahori, H.; Cardoso, S.; Tatman, D.; Lin, S.; Noss, L.; Seely, G. R.; Sereno, L.; Silber, C.; Moore, T. A.; Moore, A. L.; Gust, D. *Photochem. Photobiol.* **1995**, *62*, 1009. (b) Gust, D.; Moore, T. A.; Moore, A. L. *Res. Chem. Intermed.* **1997**, *23*, 621. (c) Yamazaki, M.; Araki, Y.; Fujitsuka, M.; Ito, O. *J. Phys. Chem. A* **2001**, *105*, 8615. (d) González, S.; Herranz, M. A.; Illescas, B.; Segura, J. L.; Martín, N. *Synth. Met.* **2001**, *121*, 1131.
- (10) (a) Williams, R. M.; Zwier, J. M.; Verhoeven, J. W. *J. Am. Chem. Soc.* **1995**, *117*, 4093. (b) Williams, R. M.; Koeberg, M.; Lawson, J. M.; An, Y.-Z.; Rubin, Y.; Paddon-Row, M. N.; Verhoeven, J. *Org. Chem.* **1996**, *61*, 5055. (c) Thomas, K. G.; Biju, V.; George, M. V.; Guldi, D. M.; Kamat, P. V. *J. Phys. Chem. A* **1998**, *102*, 5341. (d) Thomas, K. G.; Biju, V.; Guldi, D. M.; Kamat, P. V.; George, M. V. *J. Phys. Chem. B* **1999**, *103*, 8864. (e) Thomas, K. G.; Biju, V.; Guldi, D. M.; Kamat, P. V.; George, M. V. *J. Phys. Chem. A* **1999**, *103*, 10755. (f) Komamine, S.; Fujitsuka, M.; Ito, O.; Moriawaki, K.; Miyata, T.; Ohno, T. *J. Phys. Chem. A* **2000**, *104*, 11497.
- (11) (a) Liddell, P. A.; Kuciasauskas, D.; Sumida, J. P.; Nash, B.; Nguyen, D.; Moore, A. L.; Moore, T. A.; Gust, D. *J. Am. Chem. Soc.* **1997**, *119*, 1400. (b) Imahori, H.; Yamada, K.; Hasegawa, M.; Taniguchi, S.; Okada, T.; Sakata, Y. *Angew. Chem., Inter. Ed. Engl.* **1997**, *36*, 2626. (c) Luo, C.; Guldi, D. M.; Imahori, H.; Tamaki, K.; Sakata, Y. *J. Am. Chem. Soc.* **2000**, *122*, 6535. (d) Imahori, H.; Tamaki, K.; Guldi, D. M.; Luo, C.; Fujitsuka, M.; Ito, O.; Sakata, Y.; Fukuzumi, S. *J. Am. Chem. Soc.* **2001**, *123*, 2607. (e) Imahori, H.; Guldi, D. M.; Tamaki, K.; Yoshida, Y.; Luo, C.; Sakata, Y.; Fukuzumi, S. *J. Am. Chem. Soc.* **2001**, *123*, 6617. (f) Imahori, H.; Tamaki, K.; Guldi, D. M.; Luo, C.; Fujitsuka, M.; Ito, O.; Sakata, Y.; Fukuzumi, S. *J. Am. Chem. Soc.* **2001**, *123*, 2607. (g) Imahori, H.; Tamaki, K.; Araki, Y.; Sekiguchi, Y.; Ito, O.; Sakata, Y.; Fukuzumi, S. *J. Am. Chem. Soc.* **2002**, *124*, 5165. (h) Liddell, P. A.; Kodis, G.; Moore, A. L.; Moore, T. A.; Gust, D. *J. Am. Chem. Soc.* **2002**, *124*, 7668.
- (12) (a) Linssen, T. G.; Durr, K.; Hannack, M.; Hirsh, A. *J. Chem. Soc. Chem. Commun.* **1995**, 103. (b) Durr, K.; Fiedler, S.; Linssen, T.; Hirshi, A.; Hanack, M. *Chem. Ber.* **1997**, *130*, 1375. (c) Saster, A.; Gouloumis, A.; Vazquez, P.; Torres, T.; Doan, V.; Schwartz, B. J.; Wudl, F.; Echigoyen, L.; Rivera, J. *Org. Lett.* **1999**, *1*, 1807. (d) Martínez-Díaz, M. V.; Fender, N. S.; Rodríguez-Morgade, M. S.; Gomes-Lopes, M.; Dietrich, F.; Echigoyen, L.; Stoddart, J. F.; Torres, T. *J. Mater. Chem.* **2002**, *12*, 2095. (e) Guldi, D. M.; Ramey, J.; Martínez-Díaz, M. V.; de la Escosura, A.; Torres, T.; Da Ros, T.; Prato, M. *Chem. Comm.* **2002**, 2774.
- (13) (a) Sacrifici, N. S.; Wudl, F.; Heeger, A. J.; Maggini, M.; Scorrano, G.; Prato, M.; Bourassa, J.; Ford, P. C.; *Chem. Phys. Lett.* **1995**, *247*, 210. (b) Maggini, M.; Guldi, D. M.; Mondini, S.; Scorrano, G.; Paolucci, F.; Ceroni, P.; Roffia, S. *Chem. Eur. J.* **1998**, *4*, 1992. (c) Maggini, M.; Dono, A.; Scorrano, G.; Prato, M. *J. Chem. Soc. Chem. Commun.* **1998**, 845.
- (14) (a) Guldi, D. M.; Maggini, M.; Scorrano, G.; Prato, M. *J. Am. Chem. Soc.* **1997**, *119*, 974. (b) D'Souza, F.; Zandler, M. E.; Smith, P. M.; Deviprasad, G. R.; Arkady, K.; Fujitsuka, M.; Ito, O. *J. Phys. Chem. A* **2002**, *106*, 649. (c) Zandler, M. E.; Smith, P. M.; Fujitsuka, M.; Ito, O.; D'Souza, F. *J. Org. Chem.* **2002**, *67*, 9122. (d) Fujitsuka, N.; Tsuboya, R.; Hamasaki, M.; Ito, S.; Onodera, S.; Ito, O.; Yamamoto, Y. *J. Phys. Chem. A* **2003**, *107*, 1452.
- (15) (a) Martín, N.; Sánchez, L.; Herranz, M. A.; Guldi, D. M. *J. Phys. Chem. A* **2000**, *104*, 4648. (b) Herranz, M. A.; Ollescas, B.; Martín, N.; Luo, C.; Guldi, D. M. *J. Org. Chem.* **2000**, *65*, 5728. (c) Martín, N.; Sánchez, L.; Guldi, D. M. *Chem. Commun.* **2000**, 113. (d) Martín, N.; Sánchez, L.; Illescas, B.; González, S.; Herranz, M. A.; Guldi, D. M. *Carbon* **2000**, *38*, 1577. (e) Martín, N.; Sánchez, L.; Guldi, D. M. *Chem. Commun.* **2000**, 113. (f) Allard, E.; Cousseau, J.; Oruduna, J.; Garin, J.; Luo, H.; Araki, Y.; Ito, O. *Phys. Chem. Chem. Phys.* **2002**, *4*, 5944. (g) Kreher, D.; Hudhomme, P.; Gorgues, A.; Luo, H.; Araki, Y.; Ito, O. *Phys. Chem. Chem. Phys.* **2003**, *5*, 4583. (h) Sánchez, L.; Pérez, I.; Martín, N.; Guldi, D. M. *Chem. Eur. J.* **2003**, *9*, 2457.
- (16) (a) Yamashiro, T.; Aso, Y.; Otsubo, T.; Tang, H.; Harima, T.; Yamashita, K. *Chem. Lett.* **1999**, 443. (b) Fujitsuka, M.; Ito, O.; Yamashiro, T.; Aso, Y.; Otsubo, T. *J. Phys. Chem. A* **2000**, *104*, 4876. (c) Hirayama, D.; Yamashiro, T.; Takiyama, K.; Aso, Y.; Otsubo, T.; Norieda, H.; Imahori, H.; Sakata, Y. *Chem. Lett.* **2000**, 570. (d) van Hal, P. A.; Knol, J.; Langeveld-Voss, B. M. W.; Meskers, S. C. J.; Hummelen, J. C.; Janssen, R. A. J. *J. Phys. Chem. A* **2000**, *104*, 5974. (e) Fujitsuka, M.; Matsumoto, K.; Ito, O.; Yamashiro, T.; Aso, Y.; Otsubo, T. *Res. Chem. Intermed.* **2001**, *27*, 73. (f) van Hal, P. A.; Beckers, E. H. A.; Meskers, S. C. J.; Janssen, R. A. J.; Jousseme, B.; Blanchard, P.; Roncali, J. *Chem. Eur. J.* **2002**, *8*, 5415. (g) Beckers, E. H. A.; van Hal, P. A.; Dhanabalan, A.; Meskers, S. C. J.; Knol, J.; Hummelen, J. C.; Janssen, R. A. J. *J. Phys. Chem. A* **2003**, *107*, 6218.
- (17) (c) Imahori, H.; Tamaki, K.; Araki, Y.; Hasobe, T.; Ito, O.; Shimomura, A.; Kundu, S.; Okada, T.; Sakata, Y.; Fukuzumi, S. *J. Phys. Chem. A* **2002**, *106*, 1465.
- (18) Luo, H.; Fujitsuka, M.; Araki, Y.; Ito, O.; Padmawar, P.; Chiang, L. Y. *J. Phys. Chem. B* **2003**, *107*, 9312.
- (19) Yamanaka, K.; Fujitsuka, M.; Araki, Y.; Ito, O.; Aoshima, T.; Fukushima, T.; Miyashi, T. *J. Phys. Chem. A* **2004**, *108*, 250.
- (20) (a) Raimundo, J.-M.; Blanchard, P.; Brisset, H.; Akoudad, S.; Roncali, J. *Chem. Commun.* **2000**, 939. (b) Akhtaruzzaman, M.; Tomura, M.; Zaman, M. B.; Nishida, J.; Yamashita, Y. *J. Org. Chem.* **2002**, *67*, 7813. (c) Edelmann, M. J.; Raimundo, J.-M.; Utesch, N. F.; Diederich, F.; Boudon, C.; Gisselbrecht, J.-P.; Gross, M. *Helv. Chim. Acta* **2002**, *85*, 2195.
- (21) Thomas, K. R. J.; Lin, M. Velusamy, J. T.; Tao, Y.-T.; Chuen, C.-H. *Adv. Funct. Mater.* **2004**, *14*, 83.
- (22) (a) Kitamura, C.; Tanaka, S.; Yamashita, Y. *Chem. Mater.* **1996**, *8*, 570. (b) van Mullekom, H. A. M.; Vekemans, J. A. J. M.; Meijer, E. W. *Chem. Eur. J.* **1998**, *4*, 1235. (c) Banguy, C. G.; Evans, U.; Myrick, M. L.; Bunz, U. H. F. *Macromolecules* **2001**, *34*, 7592. (d) Niu, Y.-H.; Huang, J.; Cao, Y. *Adv. Mater.* **2003**, *15*, 807.
- (23) Zhang, X.; Gorohmaru, H.; Kadowaki, M.; Kobayashi, T.; Ishi-i, T.; Thiemann, T.; Mataka, S. *J. Mater. Chem.* **2004**, *14*, 1901.
- (24) Kato, S.; Matsumoto, T.; Ishi-i, T.; Thiemann, T.; Shigeiwa, M.; Gorohmaru, H.; Maeda, S.; Yamashita, Y.; Mataka, S. *Chem. Commun.* **2004**, 2342.
- (25) The MO calculation in the present study revealed that the LUMO level of the BTD moiety is slightly higher than that of the C<sub>60</sub> moiety in C<sub>60</sub>-BTD-TPA.
- (26) (a) Marcus, R. A. *J. Chem. Phys.* **1956**, *24*, 966. (b) Marcus, R. A. *J. Chem. Phys.* **1965**, *43*, 679. (c) Marcus, R. A.; Sutin, N. *Biochim. Biophys. Acta* **1985**, *811*, 265.
- (27) (a) Maggini, M.; Scorrano, G.; Prato, M. *J. Am. Chem. Soc.* **1993**, *115*, 9798. (b) Prato, M.; Maggini, M. *Acc. Chem. Res.* **1998**, *31*, 519. (c) Prato, M.; Maggini, M.; Giacometti, C.; Scorrano, G.; Sandonà, G.; Farnia, G. *Tetrahedron* **1996**, *52*, 5221.
- (28) Frich, M. J.; Truck, G. W.; Schlegel, H. B.; Scuseria, G. E.; Robb, M. A.; Cheeseman, J. R.; Zakrzewski, V. G.; Montgomery, J. A., Jr.; Stratmann, R. E.; Burant, J. C.; Dapprich, S.; Millam, J. M.; Daniels, A. D.; Kudin, K. N.; Strain, M. C.; Farkas, O.; Tomasi, J.; Barone, V.; Cossi, M.; Cammi, R.; Mennucci, B.; Pomelli, C.; Adamo, C.; Clifford, S.;

Ochterski, J.; Petersson, G. A.; Ayala, P. Y.; Cui, Q.; Morokuma, K.; Malick, D. K.; Rabuck, A. D.; Raghavachari, K.; Foresman, J. B.; Cioslowski, J.; Ortiz, J. V.; Baboul, A. G.; Stefanov, B. B.; Liu, G.; Liashenko, A.; Piskorz, P.; Komaromi, I.; Gomperts, R.; Martin, R. L.; Fox, D. J.; Keith, T.; Al-Laham, M. A.; Peng, C. Y.; Nanayakkara, A.; Gonzalez, C.; Challacombe, M.; Gill, P. M. W.; Johnson, B.; Chen, W.; Wong, M. W.; Andres, J. L.; Gonzalez, C.; Head-Gordon, M.; Replogle, E. S.; Pople, J. A. *Gaussian* 98, revision A.7; Gaussian, Inc.: Pittsburgh, PA, 1998.

(29) Weller, A. Z. *Phys. Chem. Neue Folge* **1982**, 133, 93.

(30) (a) Arbogast, J. W.; Foote, C. S.; Kao, M. J. *Am. Chem. Soc.* **1992**, 114, 2277. (b) Biczok, L.; Linschitz, H. *Chem. Phys. Lett.* **1992**, 195, 339. (c) Nonell, S.; Arbogast, J. W.; Foote, C. S. *J. Phys. Chem.* **1992**, 96, 4169. (d) Steren, C. A.; von Willigen, H.; Biczok, L.; Gupta, N.; Linschitz, H. *J. Phys. Chem.* **1996**, 100, 8920. (e) Luo, C.; Fujitsuka, M.; Watanabe, A.; Ito, O.; Gan, L.; Huang, Y. Huang, C.-H. *J. Chem. Soc., Faraday Trans.* **1998**, 94, 527.

(31) Kemp, T. J.; Martins, L. J. A. *J. Chem. Soc., Faraday Trans.* **1981**, 177, 1425.

(32) The energy levels of the lowest singlet excited states of BTD-TPA were evaluated from the fluorescence peaks, because it was difficult to evaluate the 0–0 transition due to large Stokes shift.

(33) In the excited CT state ((BTD)<sup>δ(•-)</sup>-TPA<sup>δ(•+)</sup>), contribution of the dative structure may increase comparing with that in the ground state, but considerably less than the CS state (BTD<sup>•-</sup>-TPA<sup>•+</sup>).

(34) (a) Sension, R. J.; Phillips, C. M.; Szarka, A. Z.; Romanow, W. J.; McGhie, A. R.; McCauly, J. P., Jr.; Smith, A. B., III; Hochstrasser, R. M. *J. Phys. Chem.* **1991**, 95, 6075. (b) Ebbesen, T. W.; Tanigaki, K.; Kuroshima, S. *Chem. Phys. Lett.* **1991**, 181, 501. (c) Lee, M.; Song, O.-K.; Seo, J.-C.; Kim, D.; Suh, Y. D.; Jin, S. M.; Kim, S. K. *Chem. Phys. Lett.* **1992**, 196, 325. (d) Watanabe, A.; Ito, O.; Watanabe, M.; Saito, H.; Koishi, M. *J. Chem. Soc., Chem. Commun.* **1996**, 117.

(35) Although there are some possibilities to interpret such a minor slow component, one can consider the reversible process between <sup>1</sup>C<sub>60</sub><sup>\*</sup>-BTD-TPA and intermediate state before C<sub>60</sub><sup>•-</sup>-(BTD-TPA)<sup>•+</sup>.<sup>15g</sup> Such contribution, however, is smaller 15% as shown in Figure 8.

(36) The fluorescence of BTD-TPA in toluene showed rise in the initial time (0–300 ps) followed by the slow decay. The initial rise may be related to the twisting between the BTD and TPA planes in the excited state.<sup>25</sup>

(37) In transient absorption spectra and time profiles in PhCN (Supporting Information (Figure S4), slow rise of the C<sub>60</sub><sup>•-</sup> in PhCN was observed, probably due to the intermolecular electron transfer. Thus, the transient spectra in long time scale may contain both the radical ion pairs produced via intra- and intermolecular ET processes in PhCN.

(38) (a) Jornter, J. *J. Chem. Phys.* **1976**, 64, 4860. (b) Liang, N.; Miller, J. R.; Closs, G. L. *J. Am. Chem. Soc.* **1990**, 112, 5353. (c) Chen P.; Mecklenburg, L.; Meyer, T. J. *J. Phys. Chem.* **1993**, 97, 13126. (d) Smitha, M. A.; Gopidas, K. P., *Chem. Phys. Lett.* **2001**, 350, 86. (e) May, V.; Kuhn, O. *Charge and Energy Transfer Dynamics in Molecular Systems*, 2nd ed.; Wiley-VCH: Weinheim, 2004; Chapter 6.

(39) Sandanayaka, S. D. A.; Sasabe, H.; Araki, Y.; Furusho, Y.; Ito, O.; Takata, T. *J. Phys. Chem. A* **2004**, 108, 5145.

(40) (a) Ohkubo, K.; Imahori, H.; Shao, J.; Ou, Z.; Kadesh, K. M.; Chen, Y.; Zheng, G.; Pandey, R. K.; Fujitsuka, M.; Ito, O.; Fukuzumi, S. *J. Phys. Chem. A* **2002**, 106, 10991. (b) Ohkubo, K.; Kotani, H.; Shao, J.; Ou, Z.; Kadesh, K. M.; Li, G.; Pandey, R. K.; Fujitsuka, M.; Ito, O.; Imahori, H.; Fukuzumi, S. *Angew. Chem., Int. Ed.* **2004**, 43, 853.

(41) Pilgram, K.; Zupan, M.; Skiles, R. *J. Heterocycle Chem.* **1970**, 7, 629.

(42) (a) Watanabe, N.; Kihara, N.; Furusho, Y.; Takata, T.; Araki, Y.; Ito, O. *Angew. Chem., Int. Ed.* **2003**, 42, 681. (b) Choi, M. S.; Aida, T.; Luo, H.; Y. Araki, Y.; Ito, O. *Angew. Chem., Int. Ed.* **2003**, 42, 4060. (c) Nishikawa, H.; Kojima, S.; Kodama, T.; Ikemoto, I.; Suzuki, S.; Kikuchi, K. Fujitsuka, M. Luo, H.; Araki, Y.; Ito, O. *J. Phys. Chem. A* **2004**, 108, 1881. (d) Makinoshima, T.; Fujitsuka, M.; Sasaki, M.; Araki, Y.; Ito, O.; Ito, S.; Morita, N. *J. Phys. Chem. A* **2004**, 108, 368.

(43) (a) Ito, O.; Sasaki, Y.; Yoshikawa, Y.; Watanabe, A. *J. Phys. Chem.* **1995**, 99, 9838. (b) Ito, O.; *Res. Chem. Intermed.* **1997**, 23, 389. (c) Yahata, Y.; Sasaki, Y.; Fujitsuka, M.; Ito, O. *J. Photosci.* **1999**, 6, 117.